Test-retest variability of [^{11}C]ABP688 estimates of metabotropic glutamate receptor subtype 5 availability in humans

Kelly Smart[a], Sylvia M.L. Cox[a], Atsuko Nagano-Saito[a], Pedro Rosa-Neto [b,c], Marco Leyton [a,b], and Chawki Benkelfat[a,b§].

[a] Department of Psychiatry, McGill University, 1033 Pine Ave W, Montreal, Quebec, Canada, H3A 1A1.

[b] Department of Neurology and Neurosurgery, McGill University, Montreal Neurological Institute, 3801 University Ave, Montreal, Quebec, Canada, H3A 2B4.

[c] Translational Neuroimaging Laboratory, McGill University Research Centre for Studies in Aging, 6825 Boulevard LaSalle, Verdun, Quebec, Canada, H4H 1R3.

[§] To whom correspondence should be addressed:

Kelly Smart

Phone: 514-398-8595

Fax: 514-398-4370

kelly.smart@mail.mcgill.ca

Acknowledgments:

The authors thank the personnel at the McConnell Brain Imaging Centre for technical assistance. The work in this analysis was supported by an operating grant to CB and ML from the Canadian Institutes of Health Research (CIHR, MOP-119509). The funding source had no role in study design; in the collection, analysis and interpretation of data; in the writing of the report; or in the decision to submit the article for publication.

Conflict of Interest Statement:

The authors state that they have no conflict of interest to declare.

Abstract

[^{11}C]ABP688 is a positron emission tomography (PET) radioligand that binds selectively to metabotropic glutamate type 5 receptors (mGluR5). The use of this tracer has identified receptor binding changes in clinical populations, and has been informative in drug occupancy studies. However, previous studies have found significant increases in [^{11}C]ABP688 binding in the later scan of same-day comparisons, and estimates of test-retest reliability under consistent scanning conditions are not available. The objective of this study was to assess the variability of [^{11}C]ABP688 binding in healthy people in scans performed at the same time of day. Two [^{11}C]ABP688 scans were acquired in eight healthy volunteers (6 women, 2 men) using a high-resolution research tomograph (HRRT). Scans were acquired 3 weeks apart with start times between 10:00am and 1:30pm. Mean mGluR5 binding potential (BP_{ND}) values were calculated across cortical, striatal and limbic brain regions. Participants reported on subjective mood state after each scan and blood samples were drawn for cortisol analysis. No significant change in BP_{ND} between scans was observed. Variability in BP_{ND} values of 11 to 21% was observed across regions, with the greatest change in the hippocampus and amygdala. Reliability was low to moderate. BP_{ND} was not statistically related to scan start time, subjective anxiety, serum cortisol levels, or menstrual phase in women. Overall, [^{11}C]ABP688 BP_{ND} estimates show moderate variability in healthy people. Reliability is fair in cortical and striatal regions, and lower in limbic regions. Future research using this ligand should account for this in study design and analysis.

Keywords: [^{11}C]ABP688, positron emission tomography, metabotropic glutamate receptor type 5, test-retest

Introduction

The positron emission tomography (PET) radiotracer 3-((6-methylpyridin-2-yl)ethynyl)cyclo-hex-2-en-1-one-O[^{11}C]methyloxime ([^{11}C]ABP688) binds selectively at an allosteric site on the type 5 metabotropic glutamate receptor (mGluR5) (Ametamey et al., 2006). Throughout the brain, these receptors are involved in regulating glutamatergic neurotransmission and synaptic plasticity, contributing to associative learning and memory (Anwyl, 1999; Ayala et al., 2009). mGluR5 alterations are linked to a range of psychiatric and neurological disorders (Davis et al., 2017; Esterlis et al., 2017; Scharf et al., 2015; Smart et al., 2017), while drugs targeting the radioligand binding site are being investigated for diverse conditions, including substance use disorders, fragile X syndrome, and levodopa-induced dyskinesia in Parkinson's disease (Caprioli et al., 2017; Haass-Koffler et al., 2017; Tison et al., 2013; Youssef et al., 2018). The ligand also has applications in drug development to estimate occupancy at the modulatory site (Kågedal et al., 2013; Mathews et al., 2014).

Variation in [^{11}C]ABP688 binding between subjects is considerable, with over two-fold differences in cortical binding among healthy people (DuBois et al., 2016). Compared to these healthy individuals, people with mood and substance use disorders (Akkus et al., 2013; Deschwanden et al., 2011; Esterlis et al., 2017; Martinez et al., 2014; Milella et al., 2014) are reported to have altered [^{11}C]ABP688 binding. While results in clinical populations are commonly interpreted to reflect changes in receptor density, drug challenge studies in animals and humans have raised the possibility that [^{11}C]ABP688 may also be sensitive to changes in extracellular glutamate levels. In humans, lower [^{11}C]ABP688 binding is seen following administration of ketamine, known to increase glutamate levels (DeLorenzo et al., 2015; Esterlis

et al., 2017), while binding levels increase in rats after administration of ceftriaxone, which decreases glutamate (Zimmer et al., 2015). Because [^{11}C]ABP688 binds at an allosteric site, this would not be caused by direct competition between glutamate and the radiotracer; rather, increased glutamate levels might instead alter affinity at the allosteric site or induce receptor internalization.

[^{11}C]ABP688 has shown good test-retest stability in rodents and non-human primates (DeLorenzo et al., 2011b; Elmenhorst et al., 2012; Miyake et al., 2011). In humans, however, same-day test-retest studies have found variability of up to 40% across regions (DeLorenzo et al., 2017, 2011a) following a consistent pattern of increased [^{11}C]ABP688 binding during afternoon scans relative to morning scans. The causes of this variation are unknown, but it could be related to physiological or psychological factors that differ between scans, such as circadian variation in glutamate system activity (Elmenhorst et al., 2016) or stress associated with the first scan.

Systematic variation from morning to afternoon scans in previous studies precludes accurate assessment of the amount of within-subjects variation expected under consistent scanning conditions in humans. This information is necessary in order to interpret the effects of a drug challenge and longitudinal data. Thus, the objective of the current study was to assess the test-retest reliability of [^{11}C]ABP688 binding in healthy people in scans performed three weeks apart under similar conditions.

Materials and Methods

Participants

Healthy volunteers between the ages of 20 and 40 were eligible for this study. Nine people participated. Since one scan was excluded due to low tracer specific activity, the final analyses included eight participants: two men and six women, mean age 23.7±3.8 years (range 20-34 years). Participants were physically healthy, medication-free, and had no personal or first-degree relative history of psychiatric disorders, including but not limited to mood, anxiety, or substance use disorders. All were non-smokers. Personal and family medical history were assessed in screening sessions using the Structured Clinical Interview for DSM-IV, Non-Patient edition (First et al., 2002), a medical examination by a physician, and routine blood work. Urine drug screens and pregnancy tests were obtained during screening and prior to each PET session (Express Diagnostics, MN, USA), and participants were excluded if they tested positive for illicit or recreational drugs (amphetamine, benzodiazepines, buprenorphine, cannabis, cocaine, 3,4-methylenedioxymethamphetamine, methamphetamine, methadone, or opioids). The study was carried out in accordance with the Declaration of Helsinki and approved by the Research Ethics Board of the Montreal Neurological Institute, McGill University. All participants provided written informed consent.

Study Overview

Participants underwent two [^{11}C]ABP688 brain PET scans acquired three weeks apart between 10:00am and 1:20pm. With two exceptions due to tracer production delays, scan start times for each participant were within approximately one hour of each other. Participants abstained from alcohol and caffeine for 12 hours and from food for 3 hours prior to the scan. Scans were

performed as part of a larger protocol that involved double-blind administration of *d*-amphetamine or placebo following the PET scans; participants described herein made up the placebo group. After each scan, they were moved to a separate testing facility, were administered placebo capsules, and underwent non-invasive behavioural testing for 3 hours consisting of heart rate and blood pressure measurements, pencil-and-paper questionnaires, and motor activity measures. Between scan days, participants undertook two more sessions involving a sham PET scan (lying motionless in the scanner for one hour with an intravenous catheter inserted but no tracer injected) and the same behavioural measures.

Mood and physiological measurements

Participants provided subjective ratings of anxiety (Visual Analog Scales (Bond and Lader, 1974), 0-10) after each PET scan. Date of last menstrual period and length of menstrual cycle were provided by female participants at the first scan session. This information was used to determine menstrual phase at the time of each scan. Blood samples were drawn after each scan for analysis of serum cortisol and, in four women, plasma follicle stimulating hormone (FSH) and luteinizing hormone (LH). FSH and LH levels were used to confirm menstrual phase.

Imaging Acquisition

[^{11}C]ABP688 was synthesized as described previously (Elmenhorst et al., 2010). [^{11}C]CH_3I was generated via either wet method (Jolly et al., 2017) or dry method (Synthra module). Scans were performed on a high-resolution research tomograph (HRRT) PET scanner (Siemens/CTI), which has a spatial resolution between 2.3-3.4mm full width at half maximum. A six-minute transmission scan was acquired using a ^{137}Cs point source for attenuation correction.

Immediately following this, 370MBq [^{11}C]ABP688 was administered as a 1-min bolus injection to the participant's antecubital vein. A 60-minute emission scan was initiated concurrent with the beginning of the injection. Participants were instructed to remain awake and rest quietly during the scan. Dynamic data was collected with the scanner in list mode, binned into 26 time frames (frame duration: 6 x 30s, 4 x 60s, 8 x 120s, 3 x 240s, 5 x 300s). Data were reconstructed as previously described (Milella et al., 2014) using an ordered subset expectation maximization algorithm with resolution recovery, frame realignment and motion correction to the transmission scan, and correction for random events, attenuation, scatter, dead time, decay, and intensity normalization.

High-resolution (1mm) T1-weighted magnetic resonance imaging (MRI) scans were acquired on each participant for anatomical co-registration using either a 1.5T Siemens Sonata scanner (5 participants, gradient echo pulse sequence, repetition time = 9.7ms, echo time = 4ms, flip angle = 12 º, field of view = 250mm and matrix = 256 x 256) or a 3T Siemens Trio TIM scanner (3 participants, MPRAGE sequence, repetition time = 2300ms, echo time = 3.42ms, flip angle = 9º, field of view = 256mm and matrix = 256 x 256; 1mm resolution).

Image Analysis

Binding potential, non-displaceable (BP_{ND}) values were computed relative to nonspecific binding in cerebellar grey matter using the simplified reference tissue model (SRTM) (Lammertsma and Hume, 1996), which shows high correspondence ($R^2 = 0.94$) with values calculated from 2-tissue compartment modelling methods using arterial sampling (Milella et al., 2011).

MR images were pre-processed with the CIVET pipeline version 2.0.0 (http://www.bic.mni.mcgill.ca/ServicesSoftware/CIVET/) (Zijdenbos et al., 2002) to correct for intensity non-uniformity and to discretely classify tissue into white matter, grey matter, and cerebrospinal fluid. Ten grey matter regions of interest (ROIs) were defined on participants' MRI using standard masks defined on the MNI152 template, registered to each individual's MRI. Three striatal subregions were defined as in (Mawlawi et al., 2001). Cingulate, insula, amygdala and hippocampus were defined from the Talairach Daemon atlas within PickAtlas software (Lancaster et al., 2000, 1997; Maldjian et al., 2003). Prefrontal cortex ROIs were drawn manually on each participant's MRI as defined in (Abi-Dargham et al., 2000). ROI masks were then applied to each summed radioactivity PET image using nonlinear registration. Time-activity curves were extracted based on ROIs in native PET space using tools developed by Turku PET Centre (http://www.turkupetcentre.net/). For each ROI, BP_{ND} values were calculated using SRTM. To capture spatially-restricted changes in BP_{ND} between scans, voxel-wise BP_{ND} maps were created in native space then registered to MNI space and blurred at 8mm full width half maximum using a Gaussian filter.

Statistical Analysis

Statistical analyses were performed using SPSS version 24 (IBM, NY, USA) and Matlab (The Mathworks Inc., MA, USA). Scan and participant characteristics were compared using paired *t* tests. Global BP_{ND} values were calculated as the mean of all studied regions in order to assess effects of tracer and scan characteristics (mass of tracer injected per kilogram bodyweight and *(E)*-isomer content, which can affect binding estimates (Kawamura et al., 2014)). Relationships between BP_{ND} and scan or participant characteristics were assessed using Pearson's r. Regional

BP_{ND} values were compared using repeated measures Session x Subregion ANOVAs for cortical (5 subregions), striatal (3 subregions), and limbic regions (2 subregions). For each subregion, percent change from scan 1 to scan 2 (($BP_{ND-2} - BP_{ND-1}$) / BP_{ND-1} * 100%) and absolute variability in BP_{ND} (| $BP_{ND-2} - BP_{ND-1}$ | / (($BP_{ND-1} + BP_{ND-2}$) / 2) * 100%) were calculated for each participant. Intraclass correlation coefficients (ICCs) were calculated for each region (Shrout and Fleiss, 1979). ICC provides a comparison of within-subject to between-subject variation and ranges from -1 (lowest reliability) to 1 (highest reliability). Finally, parametric maps of BP_{ND} were compared in voxel-wise paired *t* tests from scan 1 to scan 2 in each participant using SPM12 (Wellcome Trust Centre for Neuroimaging, http://www.fil.ion.ucl.ac.uk/spm/software/spm12/) with a significance threshold of $p<0.05$, corrected for false discovery rate.

Results

PET scan characteristics.

PET scan characteristics are presented in Table 1. There were no differences in specific activity (scan 1 mean 28.3 GBq/μmol, range 3.1–131.6 GBq/μmol; scan 2 mean 35.8 GBq/μmol, range 4.1–151.1 GBq/μmol; t=-0.49, p =0.64), tracer *(E)*-isomer content (scan 1 mean 90±4.3%, scan 2 mean 92±3.2%, t=-0.79, p=0.46), or in start time between first and second scans (t=0.43, p=0.68). No correlation was observed between global BP_{ND} and mass of [^{11}C]ABP688 injected (r=-0.48, p=0.23), percent *(E)*-isomer in the product (r=0.22, p=0.60), or scan start time (r=-0.05, p=0.90).

Test-retest reliability.

Results of the reliability analyses are summarized in Table 2. Mean variability was 15±3.2% across regions, ranging from 11% in the dorsolateral prefrontal cortex (dlPFC) to 21% in the hippocampus and amygdala. Reliability was fair in most prefrontal and striatal subregions, with ICC values between 0.4 and 0.6; the highest value (0.61) was found in the dorsolateral prefrontal cortex. Reliability was generally lower and variability was higher in limbic regions, with the lowest ICC value in the hippocampus (0.18, indicating poor reliability). Visual inspection of individual voxel-wise BP_{ND} maps and comparison of maximum voxel-wise BP_{ND} values within each region confirmed these trends, indicating that lower reliability was not accounted for by issues with ROI definition in these smaller, lower-binding regions. Individual patterns of regional BP_{ND} values are shown in Figure 1.

No significant differences were observed from test to retest in regional analyses (*p*s > 0.13). Figure 2 shows BP_{ND} maps at scan 1 and scan 2. Voxel-wise comparisons showed no regions of significant increase or decrease between scans.

Relationship to mood and physiological factors.

As we have seen in larger samples (Smart et al., 2018), BP_{ND} values were significantly higher in men compared to women in the dlPFC (t=-2.6, p=0.042) and the orbitofrontal cortex (t=-2.5, p=0.046). There were no Sex x Session interactions in the 3-way subregion by session by phase ANOVAs. In subregion by menstrual phase ANOVAs, BP_{ND} values did not vary by stage of menstrual cycle in any ROI (ps > 0.21).

Ratings of anxiety after the PET scan were significantly higher on the first scan day compared to the second (mean rating scan 1, 3.6±1.8; mean rating scan 2, 1.8±1.8; t=2.4 p=0.044). BP_{ND} values in the dlPFC were positively correlated with anxiety ratings at scan 2 (r=0.72, p=0.046), but this effect was not observed in other regions and the direction of the effect is the opposite of what might be predicted *a priori*. Anxiety ratings were higher in men than in women (t=-2.4, p=0.03) and the correlation with BP_{ND} was not significant when controlling for sex (r=0.59, p=0.17). No relationship was observed between difference in BP_{ND} and difference in anxiety levels between scans (*p*s > 0.44). Cortisol levels did not differ between scan days (t=-0.32, p=0.76) and no relationship was observed between BP_{ND} values and post-scan serum cortisol levels (ps > 0.45).

Discussion

This analysis reports test-retest variability of [^{11}C]ABP688 PET BP_{ND} assessed using SRTM in healthy volunteers scanned three weeks apart. The ligand showed moderate variability across most of the brain, with greater changes in limbic regions including the hippocampus, amygdala, and insula. In this homogenous sample of healthy volunteers, estimates of reliability were fair across most cortical and striatal regions, and poor in these limbic areas, reflecting substantial variability both within and between subjects. Variability in BP_{ND} was not explained by tracer specific activity, tracer isomer ratio, or by menstrual phase at time of scan in female participants. While there were measurable differences in participants' subjective anxiety following each scan, no relationship was observed between BP_{ND} and anxiety ratings or serum cortisol levels.

Test-retest reliability of [^{11}C]ABP688 signals in animal models is typically high, with 5 to 10% variation in BP_{ND} values and ICC values between 0.70 and 0.88 in rats (Elmenhorst et al., 2012). In anesthetized baboons, mean percent difference between scans was reported to be 11.5% (DeLorenzo et al., 2011b), while one study in monkeys found a tendency towards increases in BP_{ND} of approximately 13% at second scan in same-day test-retest experiments (Sandiego et al., 2013). The higher overall variability reported here could reflect species differences or the greater experimental control that is possible in anesthetized research animals.

In humans, one study designed to compare bolus to bolus/infusion tracer administration found very high correlations ($R^2 > 0.92$) between binding estimates acquired one week to 3 months apart (Burger et al., 2010). However, previous test-retest studies of [^{11}C]ABP688 using consistent methods have reported greater variability than we have seen here, with average

variation of 23-39% in regional BP_{ND} calculated relative to cerebellar grey matter (DeLorenzo et al., 2011a), and overall (region-averaged) change in BP_{ND} across participants of approximately -50 to 140% (DeLorenzo et al., 2017). In both cases, BP_{ND} values in these same-day studies were significantly higher during the second scan. A similar increase was seen with a second mGluR5 tracer, [^{18}F]FPEB (DeLorenzo et al., 2017). It was hypothesized that these increases could reflect differences in psychological or physiological states between the two scans. For example, higher subjective stress during the first than the second scan may have led to elevated extracellular glutamate, reducing [^{11}C]ABP688 signal through changes in receptor affinity or membrane expression. In the present study, higher subjective anxiety was reported following scan 1 relative to scan 2. Despite a tendency across regions for BP_{ND} values to increase at scan 2 (positive mean change values, Table 2), individual data presented in Figure 1 indicate both increases and decreases within participants. No significant change in BP_{ND} values was observed, nor did BP_{ND} correlate with anxiety ratings or serum cortisol measurements after controlling for sex.

Biological factors such as circadian variation in receptor availability could also play a role in tracer binding. [^{11}C]ABP688 BP_{ND} values in rats are approximately 10% higher during the sleep phase compared to the awake phase (Elmenhorst et al., 2016), which could account for some of the difference from morning to afternoon in humans (potentially also reflecting variation in glutamate levels, which are lower during sleep than waking phase in the striatum of rats (Marquez de Prado et al., 2000)). Scans conducted here were performed on separate days at approximately the same time of day, mitigating potential effects of circadian variation. Accordingly, no systematic differences were observed. However, while studies in humans seem to show a change in binding availability within daytime (waking) hours, no such change was

observed in the rodent model. This may be due to species differences in biological rhythms or the influence of general anesthesia in rodents. Further research will be necessary to determine the nature and timing of diurnal variation in mGluR5 binding in humans.

If tracer binding is affected by physiological changes in extracellular glutamate levels, then considerable variability in binding measures may be expected given the ubiquitous role of this transmitter in brain processes. It is not yet known how extracellular glutamate levels might influence [^{11}C]ABP688 binding. One possibility is that glutamate binding alters receptor conformation in a manner that reduces the affinity of the allosteric site. Alternately, agonist (glutamate) binding could lead to internalization of the receptor, reducing binding availability. Receptor internalization is thought to be a primary mechanism by which the binding of dopamine D2/D3 receptor radiotracers such as [^{11}C]raclopride is influenced by extracellular dopamine release (Laruelle, 2012).

Reductions in [^{11}C]ABP688 binding following ketamine administration have been identified in humans (DeLorenzo et al., 2015; Esterlis et al., 2017). These studies compared binding between same-day PET scans, and therefore may have underestimated the true binding reduction under drug in the second scan. Taken together, the test-retest data available for [^{11}C]ABP688 indicate that studies using this tracer should compare scans acquired at the same time of day. Further, longitudinal and drug challenge studies should include a control group or placebo condition to account for high variability in the absence of an intervention.

Importantly, these analyses assessed BP_{ND} estimates calculated relative to cerebellar grey matter. This method has important drawbacks, given that [^{11}C]ABP688 is known to exhibit some specific binding in the cerebellar grey matter, though at lower levels than in other brain regions (Kågedal et al., 2013). As demonstrated in DeLorenzo et al. (2017), this can influence outcome measure variability when binding in the reference region is altered over time; in that study, this led to underestimation of binding differences between scans with BP_{ND}. V_T, the tracer's volume of distribution in a target region, is calculated using plasma sampling and an arterial input function. This measure showed higher variability though the pattern of increased binding in afternoon scans was preserved. It cannot be determined if differences in cerebellum tracer retention between scans affected BP_{ND} estimates and variability in the present study. Future research should explore tracer reliability in scans performed under similar conditions using methods that do not require a brain reference region. Nevertheless, BP_{ND} values are highly correlated with V_T estimates made using plasma input functions without a reference region (Milella et al., 2011), indicating that this less invasive method can provide useful information, and it continues to be used in clinical populations. It is therefore beneficial to have an estimate of the variability observed with this outcome measure despite its potential limitations.

The radiotracer [^{18}F]FPEB binds at the same site on mGluR5 as [^{11}C]ABP688 and is also commonly used to study differences between psychiatric populations. Test-retest analyses have compared [^{18}F]FPEB scans performed on separate days, two days to 6 months apart, and have reported high reliability in tracer binding (Leurquin-Sterk et al., 2016; Park et al., 2015; Wong et al., 2013). The higher variability demonstrated for [^{11}C]ABP688 could reflect primarily technical (i.e., ligand-related) factors that provide unstable estimates of essentially similar biological

conditions. In this case, [^{11}C]ABP688 would be a suboptimal choice for longitudinal or drug occupancy studies. However, test-retest studies with [^{18}F]FPEB have been done with mostly male participants, while the sample studied here was mainly female. As greater test-retest binding changes in women than in men have been reported with [^{11}C]ABP688 (DeLorenzo et al., 2017), this may have contributed to the higher variability observed here. Furthermore, as discussed above, emerging evidence suggests that [^{11}C]ABP688 binding variability reflects, at least in part, true physiological variation in receptor binding availability. It is conceivable that [^{11}C]ABP688, which binds with lower affinity (Ametamey et al., 2006; Patel et al., 2007), could be more sensitive to these changes. Initial same-day test-retest analyses using [^{18}F]FPEB showed similar patterns as [^{11}C]ABP688 with lower magnitude of change (DeLorenzo et al., 2017), but the sample size was limited and this possibility remains to be explored systematically.

Conclusions

This study provides estimates of the test-retest variability of [^{11}C]ABP688 measurements of mGluR5 BP_{ND} in healthy people and has two main conclusions. First, binding variability is moderate, and lower in scans performed 3 weeks apart at the same time of day than has been reported with same-day scans. Second, reliability across the brain remains modest: lower in limbic regions, and higher in cortical and striatal regions. Future studies using this radiotracer should be carefully controlled to account for greater variability than has been reported in pre-clinical studies, and further work should be done to determine sources and mechanisms of [^{11}C]ABP688 variability in humans.

References

Abi-Dargham, A., Martinez, D., Mawlawi, O., Simpson, N., Hwang, D.R., Slifstein, M., Anjilvel, S., Pidcock, J., Guo, N.N., Lombardo, I., Mann, J.J., Van Heertum, R., Foged, C., Halldin, C., Laruelle, M., 2000. Measurement of striatal and extrastriatal dopamine D1 receptor binding potential with [^{11}C]NNC 112 in humans: validation and reproducibility. J. Cereb. Blood Flow Metab. Off. J. Int. Soc. Cereb. Blood Flow Metab. 20, 225–243. https://doi.org/10.1097/00004647-200002000-00003

Akkus, F., Ametamey, S.M., Treyer, V., Burger, C., Johayem, A., Umbricht, D., Gomez Mancilla, B., Sovago, J., Buck, A., Hasler, G., 2013. Marked global reduction in mGluR5 receptor binding in smokers and ex-smokers determined by [^{11}C]ABP688 positron emission tomography. Proc. Natl. Acad. Sci. U. S. A. 110, 737–742. https://doi.org/10.1073/pnas.1210984110

Ametamey, S.M., Kessler, L.J., Honer, M., Wyss, M.T., Buck, A., Hintermann, S., Auberson, Y.P., Gasparini, F., Schubiger, P.A., 2006. Radiosynthesis and preclinical evaluation of 11C-ABP688 as a probe for imaging the metabotropic glutamate receptor subtype 5. J. Nucl. Med. 47, 698–705.

Anwyl, R., 1999. Metabotropic glutamate receptors: electrophysiological properties and role in plasticity. Brain Res. Brain Res. Rev. 29, 83–120.

Ayala, J.E., Chen, Y., Banko, J.L., Sheffler, D.J., Williams, R., Telk, A.N., Watson, N.L., Xiang, Z., Zhang, Y., Jones, P.J., Lindsley, C.W., Olive, M.F., Conn, P.J., 2009. mGluR5 Positive Allosteric Modulators Facilitate both Hippocampal LTP and LTD and Enhance

Spatial Learning. Neuropsychopharmacology 34, 2057–2071. https://doi.org/10.1038/npp.2009.30

Bond, A., Lader, M., 1974. The use of analogue scales in rating subjective feelings. Br. J. Med. Psychol. 47, 211–218. https://doi.org/10.1111/j.2044-8341.1974.tb02285.x

Burger, C., Deschwanden, A., Ametamey, S., Johayem, A., Mancosu, B., Wyss, M., Hasler, G., Buck, A., 2010. Evaluation of a bolus/infusion protocol for ^{11}C-ABP688, a PET tracer for mGluR5. Nucl. Med. Biol. 37, 845–851. https://doi.org/10.1016/j.nucmedbio.2010.04.107

Caprioli, D., Justinova, Z., Venniro, M., Shaham, Y., 2017. Effect of Novel Allosteric Modulators of Metabotropic Glutamate Receptors on Drug Self-administration and Relapse: A Review of Preclinical Studies and Their Clinical Implications. Biol. Psychiatry. https://doi.org/10.1016/j.biopsych.2017.08.018

Davis, M.T., Holmes, S.E., Pietrzak, R.H., Esterlis, I., 2017. Neurobiology of Chronic Stress-Related Psychiatric Disorders: Evidence from Molecular Imaging Studies. Chronic Stress 1, 247054701771091. https://doi.org/10.1177/2470547017710916

DeLorenzo, C., DellaGioia, N., Bloch, M., Sanacora, G., Nabulsi, N., Abdallah, C., Yang, J., Wen, R., Mann, J.J., Krystal, J.H., Parsey, R.V., Carson, R.E., Esterlis, I., 2015. In Vivo Ketamine-Induced Changes in [(11)C]ABP688 Binding to Metabotropic Glutamate Receptor Subtype 5. Biol. Psychiatry 77, 266–275. https://doi.org/10.1016/j.biopsych.2014.06.024

DeLorenzo, C., Gallezot, J.-D., Gardus, J., Yang, J., Planeta, B., Nabulsi, N., Ogden, R.T., Labaree, D.C., Huang, Y.H., Mann, J.J., Gasparini, F., Lin, X., Javitch, J.A., Parsey, R.V., Carson, R.E., Esterlis, I., 2017. In vivo variation in same-day estimates of metabotropic glutamate receptor subtype 5 binding using [^{11}C]ABP688 and [^{18}F]FPEB. J. Cereb. Blood Flow Metab. 37, 2716–2727. https://doi.org/10.1177/0271678X16673646

DeLorenzo, C., Kumar, J.S.D., Mann, J.J., Parsey, R.V., 2011a. In vivo variation in metabotropic glutamate receptor subtype 5 binding using positron emission tomography and [^{11}C]ABP688. J. Cereb. Blood Flow Metab. 31, 2169–2180. https://doi.org/10.1038/jcbfm.2011.105

DeLorenzo, C., Milak, M.S., Brennan, K.G., Kumar, J.S.D., Mann, J.J., Parsey, R.V., 2011b. In vivo positron emission tomography imaging with [^{11}C]ABP688: binding variability and specificity for the metabotropic glutamate receptor subtype 5 in baboons. Eur. J. Nucl. Med. Mol. Imaging 38, 1083–1094. https://doi.org/10.1007/s00259-010-1723-7

Deschwanden, A., Karolewicz, B., Feyissa, A.M., Treyer, V., Ametamey, S.M., Johayem, A., Burger, C., Auberson, Y.P., Sovago, J., Stockmeier, C.A., Buck, A., Hasler, G., 2011. Reduced metabotropic glutamate receptor 5 density in major depression determined by [(11)C]ABP688 PET and postmortem study. Am. J. Psychiatry 168, 727–734. https://doi.org/10.1176/appi.ajp.2011.09111607

DuBois, J.M., Rousset, O.G., Rowley, J., Porras-Betancourt, M., Reader, A.J., Labbe, A., Massarweh, G., Soucy, J.-P., Rosa-Neto, P., Kobayashi, E., 2016. Characterization of age/sex and the regional distribution of mGluR5 availability in the healthy human brain

measured by high-resolution [(11)C]ABP688 PET. Eur. J. Nucl. Med. Mol. Imaging 43, 152–162. https://doi.org/10.1007/s00259-015-3167-6

Elmenhorst, D., Aliaga, A., Bauer, A., Rosa-Neto, P., 2012. Test-retest stability of cerebral mGluR5 quantification using [^{11}C]ABP688 and positron emission tomography in rats. Synapse 66, 552–560. https://doi.org/10.1002/syn.21542

Elmenhorst, D., Mertens, K., Kroll, T., Oskamp, A., Ermert, J., Elmenhorst, E.-M., Wedekind, F., Beer, S., Coenen, H.H., Bauer, A., 2016. Circadian variation of metabotropic glutamate receptor 5 availability in the rat brain. J. Sleep Res. 25, 754–761. https://doi.org/10.1111/jsr.12432

Elmenhorst, D., Minuzzi, L., Aliaga, A., Rowley, J., Massarweh, G., Diksic, M., Bauer, A., Rosa-Neto, P., 2010. In vivo and in vitro validation of reference tissue models for the mGluR(5) ligand [(11)C]ABP688. J. Cereb. Blood Flow Metab. 30, 1538–1549. https://doi.org/10.1038/jcbfm.2010.65

Esterlis, I., DellaGioia, N., Pietrzak, R.H., Matuskey, D., Nabulsi, N., Abdallah, C.G., Yang, J., Pittenger, C., Sanacora, G., Krystal, J.H., Parsey, R.V., Carson, R.E., DeLorenzo, C., 2017. Ketamine-induced reduction in mGluR5 availability is associated with an antidepressant response: an [^{11}C]ABP688 and PET imaging study in depression. Mol. Psychiatry. https://doi.org/10.1038/mp.2017.58

First, M.B., Spitzer, R.L., Gibbon, M., Williams, J.B.W., 2002. Structured Clinical Interview for DSM-IV-TR Axis I Disorders, Research Version. (SCIP-I/P). Biometrics Research, New York State Psychiatric Institute, New York.

Haass-Koffler, C.L., Goodyear, K., Long, V.M., Tran, H.H., Loche, A., Cacciaglia, R., Swift, R.M., Leggio, L., 2017. A Phase I randomized clinical trial testing the safety, tolerability and preliminary pharmacokinetics of the mGluR5 negative allosteric modulator GET 73 following single and repeated doses in healthy volunteers. Eur. J. Pharm. Sci. 109, 78–85. https://doi.org/10.1016/j.ejps.2017.07.031

Jolly, D., Hopewell, R., Kovacevic, M., Li, Q.Y., Soucy, J.-P., Kostikov, A., 2017. Development of "[^{11}C]kits" for a fast, efficient and reliable production of carbon-11 labeled radiopharmaceuticals for Positron Emission Tomography. Appl. Radiat. Isot. 121, 76–81. https://doi.org/10.1016/j.apradiso.2016.11.020

Kågedal, M., Cselényi, Z., Nyberg, S., Raboisson, P., Ståhle, L., Stenkrona, P., Varnäs, K., Halldin, C., Hooker, A.C., Karlsson, M.O., 2013. A positron emission tomography study in healthy volunteers to estimate mGluR5 receptor occupancy of AZD2066 - estimating occupancy in the absence of a reference region. NeuroImage 82, 160–169. https://doi.org/10.1016/j.neuroimage.2013.05.006

Kawamura, K., Yamasaki, T., Kumata, K., Furutsuka, K., Takei, M., Wakizaka, H., Fujinaga, M., Kariya, K., Yui, J., Hatori, A., Xie, L., Shimoda, Y., Hashimoto, H., Hayashi, K., Zhang, M.-R., 2014. Binding potential of (E)-[^{11}C]ABP688 to metabotropic glutamate receptor subtype 5 is decreased by the inclusion of its ^{11}C-labelled Z-isomer. Nucl. Med. Biol. 41, 17–23. https://doi.org/10.1016/j.nucmedbio.2013.09.008

Lammertsma, A.A., Hume, S.P., 1996. Simplified reference tissue model for PET receptor studies. NeuroImage 4, 153–158. https://doi.org/10.1006/nimg.1996.0066

Lancaster, J.L., Summerlin, J.L., Rainey, L., Freitas, C.S., Fox, P.T., 1997. The Talairach Daemon a database server for talairach atlas labels. Neuroimage 5(4 PART II).

Lancaster, J.L., Woldorff, M.G., Parsons, L.M., Liotti, M., Freitas, C.S., Rainey, L., Kochunov, P.V., Nickerson, D., Mikiten, S.A., Fox, P.T., 2000. Automated Talairach atlas labels for functional brain mapping. Hum. Brain Mapp. 10, 120–131.

Laruelle, M., 2012. Measuring Dopamine Synaptic Transmission with Molecular Imaging and Pharmacological Challenges: The State of the Art, in: Molecular Imaging in the Clinical Neurosciences, Neuromethods. Humana Press, Totowa, NJ, pp. 163–203. https://doi.org/10.1007/7657_2012_45.

Leurquin-Sterk, G., Postnov, A., de Laat, B., Casteels, C., Celen, S., Crunelle, C.L., Bormans, G., Koole, M., Van Laere, K., 2016. Kinetic modeling and long-term test-retest reproducibility of the mGluR5 PET tracer 18F-FPEB in human brain. Synap. N. Y. N 70, 153–162. https://doi.org/10.1002/syn.21890

Maldjian, J.A., Laurienti, P.J., Kraft, R.A., Burdette, J.H., 2003. An automated method for neuroanatomic and cytoarchitectonic atlas-based interrogation of fMRI data sets. NeuroImage 19, 1233–1239.

Marquez de Prado, B., Castañeda, T.R., Galindo, A., del Arco, A., Segovia, G., Reiter, R.J., Mora, F., 2000. Melatonin disrupts circadian rhythms of glutamate and GABA in the neostriatum of the aware rat: a microdialysis study. J. Pineal Res. 29, 209–216.

Martinez, D., Slifstein, M., Nabulsi, N., Grassetti, A., Urban, N.B.L., Perez, A., Liu, F., Lin, S.-F., Ropchan, J., Mao, X., Kegeles, L.S., Shungu, D.C., Carson, R.E., Huang, Y., 2014. Imaging glutamate homeostasis in cocaine addiction with the metabotropic glutamate receptor 5 positron emission tomography radiotracer [(11)C]ABP688 and magnetic resonance spectroscopy. Biol. Psychiatry 75, 165–171. https://doi.org/10.1016/j.biopsych.2013.06.026

Mathews, W.B., Kuwabara, H., Stansfield, K., Valentine, H., Alexander, M., Kumar, A., Hilton, J., Dannals, R.F., Wong, D.F., Gasparini, F., 2014. Dose-dependent, saturable occupancy of the metabotropic glutamate subtype 5 receptor by fenobam as measured with [^{11}C]ABP688 PET imaging. Synapse 68, 565–573. https://doi.org/10.1002/syn.21775

Mawlawi, O., Martinez, D., Slifstein, M., Broft, A., Chatterjee, R., Hwang, D.-R., Huang, Y., Simpson, N., Ngo, K., Van Heertum, R., Laruelle, M., 2001. Imaging Human Mesolimbic Dopamine Transmission With Positron Emission Tomography: I. Accuracy and Precision of D2 Receptor Parameter Measurements in Ventral Striatum: J. Cereb. Blood Flow Metab. 21, 1034–1057. https://doi.org/10.1097/00004647-200109000-00002

Milella, M., Reader, A., Albrechtsons, D., Minuzzi, L., Soucy, J., Benkelfat, C., Leyton, M., Rosa-Neto, P., 2011. Human PET validation study of reference tissue models for the mGluR5 ligand [^{11}C]ABP688. Presented at the 41st Annual Meeting of The Society for Neuroscience, Washington, DC.

Milella, M.S., Marengo, L., Larcher, K., Fotros, A., Dagher, A., Rosa-Neto, P., Benkelfat, C., Leyton, M., 2014. Limbic system mGluR5 availability in cocaine dependent subjects: a

high-resolution PET [(11)C]ABP688 study. NeuroImage 98, 195–202. https://doi.org/10.1016/j.neuroimage.2014.04.061

Miyake, N., Skinbjerg, M., Easwaramoorthy, B., Kumar, D., Girgis, R.R., Xu, X., Slifstein, M., Abi-Dargham, A., 2011. Imaging Changes in Glutamate Transmission In Vivo with the Metabotropic Glutamate Receptor 5 Tracer [^{11}C]ABP688 and N-Acetylcysteine Challenge. Biol. Psychiatry 69, 822–824. https://doi.org/10.1016/j.biopsych.2010.12.023

Park, E., Sullivan, J.M., Planeta, B., Gallezot, J.-D., Lim, K., Lin, S.-F., Ropchan, J., McCarthy, T.J., Ding, Y.-S., Morris, E.D., Williams, W.A., Huang, Y., Carson, R.E., 2015. Test-retest reproducibility of the metabotropic glutamate receptor 5 ligand [^{18}F]FPEB with bolus plus constant infusion in humans. Eur. J. Nucl. Med. Mol. Imaging 42, 1530–1541. https://doi.org/10.1007/s00259-015-3094-6

Patel, S., Hamill, T.G., Connolly, B., Jagoda, E., Li, W., Gibson, R.E., 2007. Species differences in mGluR5 binding sites in mammalian central nervous system determined using in vitro binding with [18F]F-PEB. Nuclear Medicine and Biology 34, 1009–1017. https://doi.org/10.1016/j.nucmedbio.2007.07.009

Sandiego, C.M., Nabulsi, N., Lin, S.-F., Labaree, D., Najafzadeh, S., Huang, Y., Cosgrove, K., Carson, R.E., 2013. Studies of the metabotropic glutamate receptor 5 radioligand [^{11} C]ABP688 with *N* -acetylcysteine challenge in rhesus monkeys. Synapse 67, 489–501. https://doi.org/10.1002/syn.21656

Scharf, S.H., Jaeschke, G., Wettstein, J.G., Lindemann, L., 2015. Metabotropic glutamate receptor 5 as drug target for Fragile X syndrome. Curr. Opin. Pharmacol. 20, 124–134. https://doi.org/10.1016/j.coph.2014.11.004

Shrout, P.E., Fleiss, J.L., 1979. Intraclass correlations: uses in assessing rater reliability. Psychol. Bull. 86, 420–428.

Smart, K., Cox, S.M.L., Scala, S.G., Tippler, M., Jaworska, N., Boivin, M., Séguin, J., Benkelfact, C., Leyton, M., 2018. High resolution [^{11}C]ABP688 imaging of mGluR5 in healthy volunteers: sex differences and test-retest variability. Presented at the XII International Symposium of Functional Neuroreceptor Mapping of the Living Brain, London, United Kingdom.

Smart, K., Scala, S., El Mestikawy, S., Benkelfat, C., Leyton, M., 2017. Cocaine addiction and metabotropic glutamate receptor subtype 5, in: The Neuroscience of Cocaine: Mechanisms and Treatment. Academic Press (Elsevier).

Tison, F., Durif, F., Corvol, J.C., Eggert, K., Trenkwalder, C., Lew, M., Isaacson, S., Keywood, C., Rascol, O., 2013. Safety, Tolerability and Anti-Dyskinetic Efficacy of Dipraglurant, a Novel mGluR5 Negative Allosteric Modulator (NAM) in Parkinson's Disease (PD) Patients with Levodopa-Induced Dyskinesia (LID) (S23.004). Neurology 80, S23.004.

Wong, D.F., Waterhouse, R., Kuwabara, H., Kim, J., Brašić, J.R., Chamroonrat, W., Stabins, M., Holt, D.P., Dannals, R.F., Hamill, T.G., Mozley, P.D., 2013. ^{18}F-FPEB, a PET radiopharmaceutical for quantifying metabotropic glutamate 5 receptors: a first-in-human

study of radiochemical safety, biokinetics, and radiation dosimetry. J. Nucl. Med. Off. Publ. Soc. Nucl. Med. 54, 388–396. https://doi.org/10.2967/jnumed.112.107995

Youssef, E.A., Berry-Kravis, E., Czech, C., Hagerman, R.J., Hessl, D., Wong, C.Y., Rabbia, M., Deptula, D., John, A., Kinch, R., Drewitt, P., Lindemann, L., Marcinowski, M., Langland, R., Horn, C., Fontoura, P., Santarelli, L., Quiroz, J.A., 2018. Effect of the mGluR5-NAM Basimglurant on Behavior in Adolescents and Adults with Fragile X Syndrome in a Randomized, Double-Blind, Placebo-Controlled Trial: FragXis Phase 2 Results. Neuropsychopharmacology 43, 503–512. https://doi.org/10.1038/npp.2017.177

Zijdenbos, A.P., Forghani, R., Evans, A.C., 2002. Automatic "pipeline" analysis of 3-D MRI data for clinical trials: application to multiple sclerosis. IEEE Trans. Med. Imaging 21, 1280–1291. https://doi.org/10.1109/TMI.2002.806283

Zimmer, E.R., Parent, M.J., Leuzy, A., Aliaga, Antonio, Aliaga, Arturo, Moquin, L., S Schirrmacher, E., Soucy, J.-P., Skelin, I., Gratton, A., Gauthier, S., Rosa-Neto, P., 2015. Imaging in vivo glutamate fluctuations with [^{11}C]ABP688: a GLT-1 challenge with ceftriaxone. J. Cereb. Blood Flow Metab. 35, 1169–1174. https://doi.org/10.1038/jcbfm.2015.35

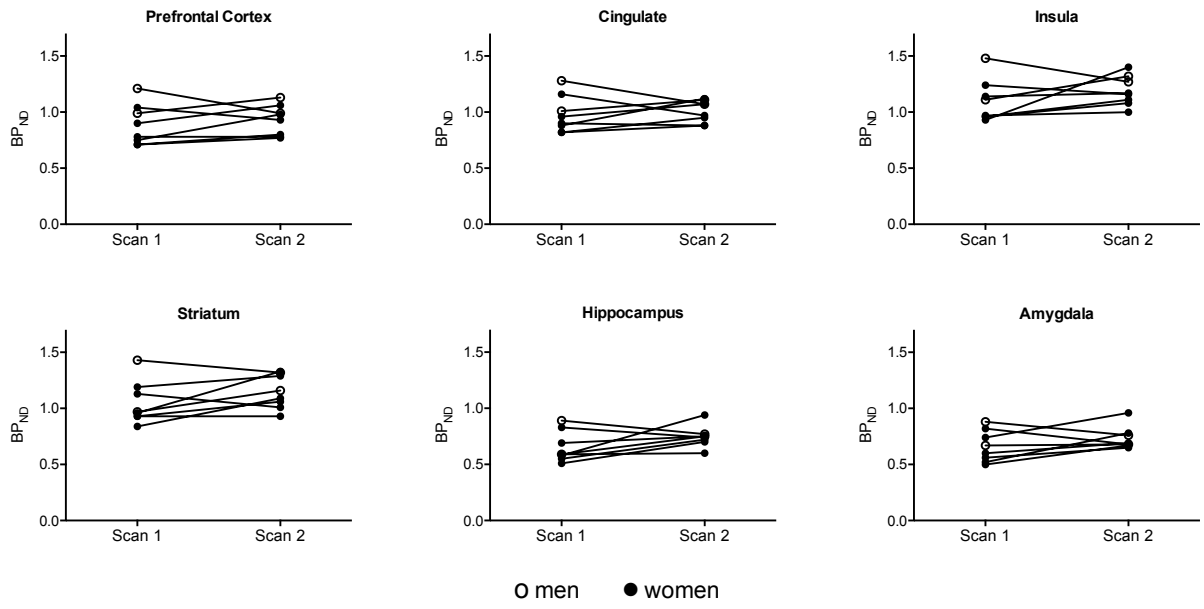

Figure 1 Individual changes in regional BP_{ND} values from scan 1 to scan 2 in 8 healthy volunteers.

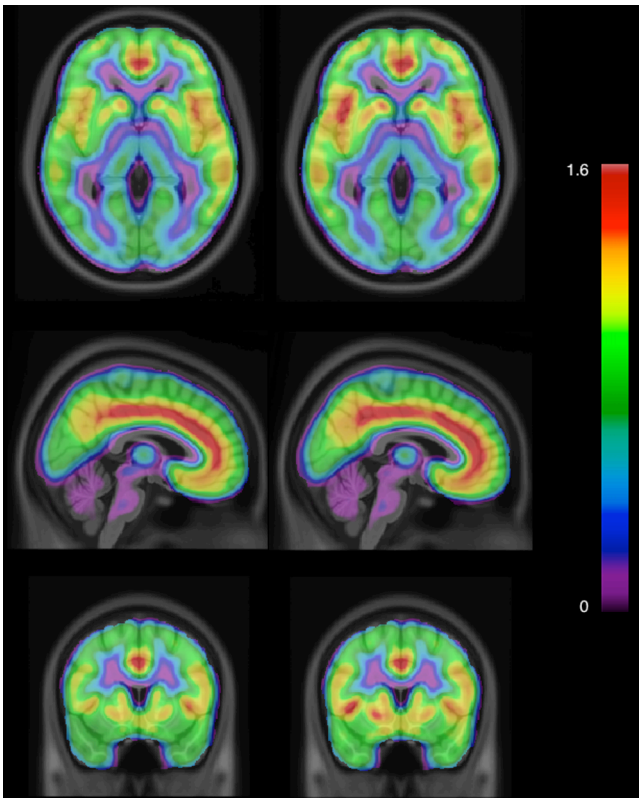

Figure 2 Average voxel-wise BP_{ND} maps at first (left) and second (right) scan overlaid on MNI152 template MRI.

Table 1 Scan information.

Participant	Time of tracer injection		Specific activity (GBq/μmol)		% *(E)*-isomer	
	Scan 1	*Scan 2*	*Scan 1*	*Scan 2*	*Scan 1*	*Scan 2*
1	10:00	10:50	11.2	5.0	80.1	94.7
2	11:05	12:09	131.6	89.3	94.3	93.2
3	10:23	11:00	17.0	7.9	90.3	85.5
4	12:35	11:13	3.1	4.1	89.9	90.1
5	10:57	11:10	6.5	6.0	88.8	93.5
6	11:04	11:07	6.6	9.4	91.0	92.2
7	13:17	11:08	7.9	13.3	92.7	94.5
8	11:17	10:39	42.6	151.1	91.8	88.8
Mean ± S.D.			28.3 ± 43.6	35.8 ± 54.8	89.9 ± 4.3	91.5 ± 3.2

Table 2 Test-retest variability for [^{11}C]ABP688 BP_{ND}.

Region	Scan 1 BP_{ND} (mean±SD)	Scan 2 BP_{ND} (mean±SD)	Mean % change	Mean absolute variability	ICC
Cortex	0.94 ± 0.17	0.99 ± 0.12	+7%	13%	0.472
Prefrontal	0.90 ± 0.18	0.95 ± 0.13	+7%	13%	0.565
mPFC	1.0 ± 0.21	1.1 ± 0.13	+6%	14%	0.544
dlPFC	0.88 ± 0.16	0.90 ± 0.13	+4%	11%	0.612
OFC	0.80 ± 0.18	0.87 ± 0.14	+11%	15%	0.529
Insula	1.0 ± 0.18	1.1 ± 0.11	+11%	14%	0.190
Cingulate	0.98 ± 0.17	1.0 ± 0.10	+5%	13%	0.360
Striatum	1.0 ± 0.19	1.1 ± 0.15	+11%	14%	0.440
Associative	1.1 ± 0.19	1.2 ± 0.15	+10%	15%	0.287
Ventral	1.2 ± 0.22	1.3 ± 0.19	+11%	14%	0.562
Sensorimotor	0.87 ± 0.18	0.96 ± 0.14	+14%	15%	0.465
Limbic subcortical	0.65 ± 0.15	0.73 ± 0.09	+15%	21%	0.224
Amygdala	0.65 ± 0.15	0.73 ± 0.10	+15%	21%	0.315
Hippocampus	0.65 ± 0.15	0.73 ± 0.11	+16%	21%	0.179

BP_{ND}, binding potential, non-displaceable; ICC, intraclass correlation coefficient; mPFC, medial prefrontal cortex; dlPFC, dorsolateral prefrontal cortex; OFC, orbitofrontal cortex.